

Space-temporal analysis of the dynamics of land coverage and use in the surroundings of the Rio de Janeiro Basin - Bahia/Brazil from biophysical parameters

Changes in land use and cover have been causing serious environmental problems in the savannah systems in the World and specifically in the Cerrado of Brazil. Studies in watersheds by remote sensing can provide information that allows detecting and evaluating changes in the land cover and use. This work aims to analyze the space-time dynamics of the Rio de Janeiro-BA watershed through the biophysical parameters NDVI (Normalized Difference Vegetation Indices), SAVI (Soil-adjusted Vegetation Indices), LAI (Leaf Area Index) and TS (Surface Temperature), estimated through spectral responses of Landsat-5 TM and Landsat-8 OLI/TIR satellite images, between the years 1984 to 2017. The results obtained to portray the various uses of land cover, highlighting the presence of native vegetation, water bodies, exposed soil, rainfed and irrigated agriculture. The relationship between energy flows in the Cerrado of the Rio de Janeiro Basin BA/Brazil proved to be representative compared to the vegetation variation in the analyzed period, favoring local and regional environmental and climatic analysis. The variation of available water in the environment, characterized a strong relationship of the seasonality in the data, reflecting directly with the changes of the indices.

Keywords: Remote sensing; Biophysical parameters; Spatio-temporal dynamics.

Análise espaço-temporal da dinâmica da cobertura e uso do solo no entorno da bacia do Rio de Janeiro - Bahia/Brasil a partir de parâmetros biofísicos

As mudanças no uso e cobertura da terra têm causado sérios problemas ambientais nos sistemas de savana no mundo e especificamente no Cerrado do Brasil. Estudos em bacias hidrográficas por sensoriamento remoto podem fornecer informações que permitem detectar e avaliar as mudanças na cobertura e uso do solo. Este trabalho visa analisar a dinâmica espaço-tempo da bacia hidrográfica do Rio de Janeiro-BA através dos parâmetros biofísicos NDVI (Normalized Difference Vegetation Indices), SAVI (Soil-adjusted Vegetation Indices), LAI (Leaf Area Index) e TS (Surface Temperature), estimados através de respostas espectrais das imagens de satélite Landsat-5 TM e Landsat-8 OLI/TIR, entre os anos de 1984 a 2017. Os resultados obtidos para retratar os diversos usos da cobertura do solo, destacando a presença de vegetação nativa, corpos d'água, solo exposto, agricultura irrigada e pluvial. A relação entre os fluxos de energia no Cerrado da Bacia do Rio de Janeiro BA/Brasil mostrou-se representativa em relação à variação da vegetação no período analisado, favorecendo as análises ambientais e climáticas locais e regionais. A variação da água disponível no ambiente, caracterizou uma forte relação da sazonalidade nos dados, refletindo diretamente com as mudanças dos índices.

Palavras-chave: Sensoriamento remoto; Parâmetros biofísicos; Dinâmica espaço-temporal.

Topic: **Geodésia, Cartografia e Sensoriamento Remoto**

Received: **05/09/2022**

Reviewed anonymously in the process of blind peer.

Approved: **22/09/2022**

Edimar Souza Dias

Universidade Federal do Oeste da Bahia, Brasil
<http://lattes.cnpq.br/7322906269065751>
edimar.s.d@hotmail.com

Elvis Bergue Mariz Moreira

Universidade Federal do Oeste da Bahia, Brasil
<http://lattes.cnpq.br/5001383251639101>
<http://orcid.org/0000-0001-6732-3005>
elvis.moreira@ufob.edu.br

Admilson da Penha Pacheco

Universidade Federal de Pernambuco, Brasil
<http://lattes.cnpq.br/2244303605944370>
<http://orcid.org/0000-0002-3635-827X>
pacheco3p@gmail.com

Jadson Freire da Silva

Universidade Federal de Pernambuco, Brasil
<http://lattes.cnpq.br/1773238385935204>
<http://orcid.org/0000-0002-1106-0688>
jadsonfreiresilva@gmail.com

Henrique dos Santos Ferreira

Universidade Federal de Pernambuco, Brasil
<http://lattes.cnpq.br/0137653754892297>
henriquehsf86@hotmail.com



DOI: 10.6008/CBPC2179-6858.2022.009.0003

Referencing this:

DIAS, E. S.; MOREIRA, E. B. M.; PACHECO, A. P.; SILVA, J. F.; FERREIRA, H. S.. Space-temporal analysis of the dynamics of land coverage and use in the surroundings of the Rio de Janeiro Basin - Bahia/Brazil from biophysical parameters. **Revista Ibero Americana de Ciências Ambientais**, v.13, n.9, p.27-42, 2022. DOI:

<http://doi.org/10.6008/CBPC2179-6858.2022.009.0003>

INTRODUCTION

The climate variability and changes in the land use and cover generate a significant impact on the processes of runoff-erosion of the Earth's surface (FONSECA et al., 2022). Changes in the land use and cover caused by the advance of agriculture have been causing serious environmental problems around the world, especially in Brazil (CUNHA et al., 2022).

This global change has significant impacts on the savannah biomes around the world. Processes related to climate change or agricultural expansion threaten the state, function, and services of the ecosystem. The Brazilian Tropical Savanna (Cerrado) is the second largest biome in South America, occupying approximately 2 million km² (ALENCAR et al., 2020). According to these authors, the Brazilian Cerrado represents the largest savanna in South America and the most threatened biome in Brazil due to agricultural expansion. Cerrado is the savanna with the greatest biological diversity in the world and is considered one of the global hotspots for the biodiversity conservation, once it is under serious human-induced threats (MITTERMEIER et al., 2011; STRASSBURG et al., 2017). Cerrado presents a large latitudinal and longitudinal variation, resulting in different ecoregions (SANO et al., 2019). In recent years, the Cerrado Biome in Brazil has faced serious environmental problems due to abrupt changes in land use and cover, causing increased soil loss, sediment production and water turbidity (CUNHA et al., 2022). Monitoring Cerrado is therefore urgently needed to assess the state of the system as well as to better analyze and understand ecosystem responses to ongoing adaptations and changes.

The Cerrado ecosystem in Bahia/Brazil is in the western region and has two ecoregions, called Chapadão do São Francisco and Depression of Paranaguá (ARRUDA et al., 2008). The Cerrado biome in western Bahia state has shown profound changes in land use and cover due to the expansion of agricultural frontiers in the recent decades (FALEIRO et al., 2009).

The western region of Bahia state underwent an intense process of agricultural expansion in the 1980s and 1990s, becoming the main agricultural frontier of the state, which became a major national producer of soybeans, corn, cotton, coffee, and fruits (MENDONÇA, 2006). According to Reis (2014), the expansion of agriculture in the region occurred after the implementation of the Japanese-Brazilian Cooperation Program for the Development of the Cerrado biomes (PRODECER), which modernized the Bahian agriculture in the late 1970s until the 1980s. Thus, causing an accelerated expansion and occupation of land in the western region of this state. Along with the advance of the land occupation, the region gained visibility of agricultural production. The Rio de Janeiro Hydrographic Basin is significant to the region, both for its tourist potential, with two waterfalls (Aba Vidas and Redondo), and for the availability of surface and underground water resources, which made possible the development of irrigated agriculture in the last few years (REIS, 2014).

The quantification and monitoring of vegetation indices and the surface temperature in watersheds, obtained from orbital data from remote sensing, have been widely used in the diagnosis of anthropic or natural changes that occur in the environmental landscape. Changes in the land use and occupation can be

identified with the increase in the surface temperature, as well as through the reduction of vegetation indices, through remote sensing observations (TARTARI et al., 2015; SILVA et al., 2019).

According to Argemiro (2018), the study of biophysical parameters of the Earth's surface, such as normalized difference vegetation index (NDVI), soil-adjusted vegetation index (SAVI), leaf area index (LAI) and surface temperature (Ts), allow the quantification and identification of patterns of environmental and/or climatic changes, whether of natural or anthropic origin.

The use of these spectral indices of vegetation has gained space in the study of different ecosystems and in the management of large areas, standing out as a good alternative for obtaining characteristics of an area on a regional scale, as they allow spectral responses of different uses on heterogeneous surfaces (LOPES et al., 2010; BEZERRA et al., 2014). According to Liu (2006), the natural causes of soil degradation are related to exposure to extreme and persistent weather events (dryness and prolonged droughts). The surface temperature is a very important parameter in the study of environmental changes, such as the monitoring of climatic conditions and the biological variations of terrestrial surfaces related to hydrology as well as in the applications of models for predicting climate change on the terrestrial surface (LIU, 2006).

Differences in the sensitivity of different vegetation indices are observed depending on the moisture status, tree cover and type of phytophysiology (OLIVEIRA et al., 2020). Thus, time series are necessary to fully capture spectral states and changes, since grassland and savannah formations present high levels of spectral and phenological variation (HILL, 2013; OLIVEIRA et al., 2020).

The 50-year history of Landsat satellite data has systematically favored several studies of environmental monitoring of the Earth's surface. The opening of the extensive data collection of the Landsat archive has facilitated different surveys of natural resources, in addition to allowing the possibility of combining data from Thematic Mapper (TM), Enhanced Thematic Mapper (ETM+) and Operational Land Imager (OLI) sensors, linked to Landsat satellites 5, 7 and 8, respectively. This improves the temporal resolution potentially to eight days, making Landsat an ingenious system for retrieving detailed phenological information and offering a great opportunity to observe vegetation gradients over long periods of time with sufficient spatial resolution.

Mapping heterogeneous ecosystems such as savannas requires spatial details as well as the ability to derive important phenological parameters for monitoring habitats or ecosystem responses to climate change. Accurate mapping and monitoring of the temporal and spatial dynamics of Cerrado vegetation are essential to understand ecosystem properties and responses to ongoing changes in processes to support the decision makers (ROCHA et al., 2011; SANO et al., 2010).

In this context, this study aims to evaluate the spatio-temporal changes in the land use and in the land cover in the Rio de Janeiro Basin - BA/Brazil from the biophysical parameters NDVI, SAVI, IAF and Surface Temperature (Ts) obtained from optical images of the Landsat-5 TM and Landsat-8 OLI-TIR satellites, in the period that comprised the years 1984, 1994, 2004 and 2017.

MATERIALS AND METHODS

The study area comprises the Rio de Janeiro Hydrographic Basin, which is a sub-basin that makes up the Rio Grande Basin. It is in the extreme western region of Bahia state, between the municipalities of Barreiras and Luís Eduardo Magalhães. It presents territorial extension between the coordinates: latitude 11°30'0"S and 12°15'0"S and longitude 45°15'0"W and 46°30'0"W, covering an area of approximately 3,813 km² (Figure 1).

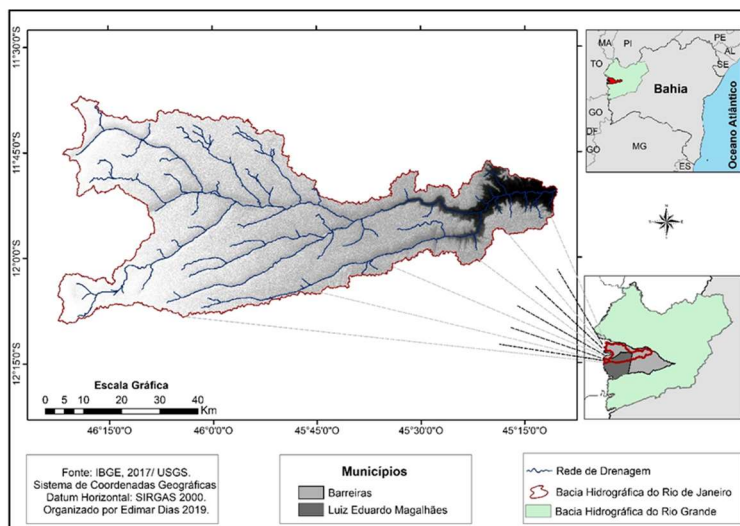


Figure 1: Location map of the Rio de Janeiro Basin – BA state.

According to the Geological Survey of Brazil - CPRM (2013), the Rio de Janeiro Hydrographic Basin is geomorphologically inserted in the sub-structural plane of the General and Structured Levels – Chapadão Ocidental do São Francisco, with flattened relief. Having as lithological structure the formations: Serra da Mamona formation; Riachão das Neves formation, both belonging to the Bambuí group (Neoproterozoic); Urucuia group (Neocretaceous) composed of sandstones, claystones and para-conglomerates; and alluvial deposits formed by gravel, sand, silt, and clay deposits (Geological Service of Brazil - CPRM, 2013).

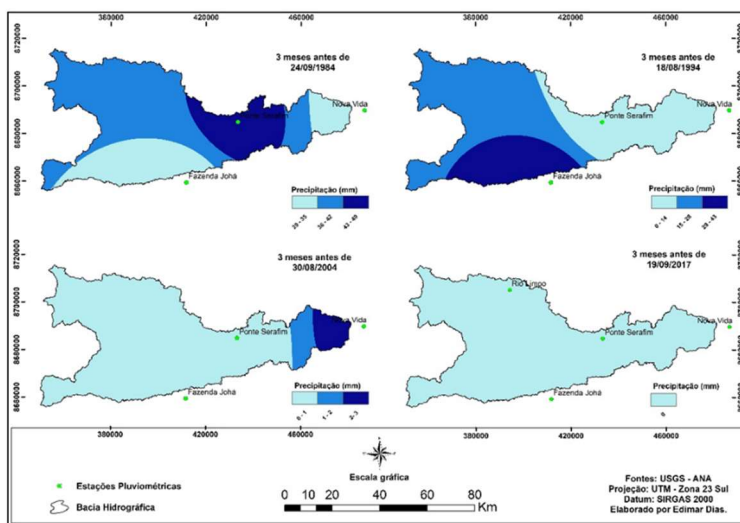


Figure 2: Map of precipitation accumulated in the three months prior to the passage of satellites in the Rio de Janeiro Hydrographic Basin on the dates under analysis.

The relief of the Rio de Janeiro basin has the highest altitudes in the western portion of the basin, with a maximum value of 913 m, and the lowest elevations are in the east, at the confluence of Rio de Janeiro with Rio Branco, with a minimum value of 471 m. The greatest slopes are found in the eastern portion, suggesting a higher velocity of water from surface runoff and, consequently, a greater vulnerability of soils to erosion. The soils of the Rio de Janeiro basin under study are classified as Red-Yellow Latosol and Quartzaren Neosol (EMBRAPA, 2010).

Figure 2 shows the map with the spatial distribution of the accumulated precipitation in the Rio de Janeiro Basin, referring to the three months prior to the passage of the Landsat-5 TM and Landsat-8 OLI/TIR satellites on the following dates: 09/24/1984; 08/18/1994; 08/30/2004 and 09/19/2017. The dates of the images comprise an interval of 33 years and the present data from similar periods, referring to the winter season. The Methodological Procedures for the development of this work are presented in the flowchart of figure 3.

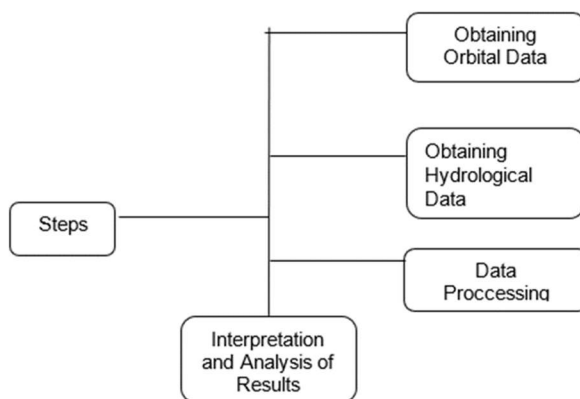


Figure 3: Flowchart of the steps.

The data required for this study were the following: 1) SRTM (Shuttle Radar Topography Mission) images with a resolution of 30 meters, used to delimit the study area and to analyze the physiographic aspects of the watershed; 2) Orbital images of the Landsat-5 TM and Landsat-8 OL/TIR satellites, orbits 220 and 221 and station 068, from the years 1984, 1994, 2004 and 2017. These data were obtained free of charge through electronic websites from the United States Geological Survey (USGS) and the National Institute for Space Research (INPE). In the case of satellite images, the scenes with the lowest percentage of cloud cover were selected. The data referring to the delimitation of the municipalities of the study area, in vector form, of the shapefile type, were obtained from the website of the Brazilian Institute of Geography and Statistics (IBGE).

The geological base as well as other physical geographic data of the study area were acquired through the website of the Brazilian Geological Service - CPRM (Public Company of Mineral Resources (Brazilian Geological Service - CPRM, 2013).

The precipitation data were obtained from the Hydrological Information System database – HIDROWEB, under the responsibility of the National Water Agency (ANA). In the selection of rainfall stations, the spatial distribution of the stations was considered, with those located in the Rio de Janeiro basin or in its vicinity being selected.

The stations selected were those that presented historical series with consistent data and with the least possible failures. The selection resulted in a dataset of four rainfall stations (Table 1).

Table 1: Rainfall stations selected for the study.

Code	Stations	Municipalities	Responsible	Operator
1145013	Ponte Serafim	Barreiras	ANA	CPRM
1145014	Nova Vida	Barreiras	ANA	CPRM
1245014	Fazenda Johá	Luiz Eduardo Magalhães	ANA	CPRM
1145024	Rio Limpo	Barreiras	ANA	CPRM

After collecting and selecting the images, they were processed in the Geographic Information System (GIS) environment using ArcGis 10.4.1 and Erdas Imagine 9.2 software, from the Geoprocessing Laboratory - LABGEO, belonging to the Federal University do Oeste da Bahia (UFOB). In the SRTM/MDE (Digital Elevation Model) images, the following processes were performed: watershed delimitation, channel hierarchy, slope, altitude, area, and perimeter (Figure 4).

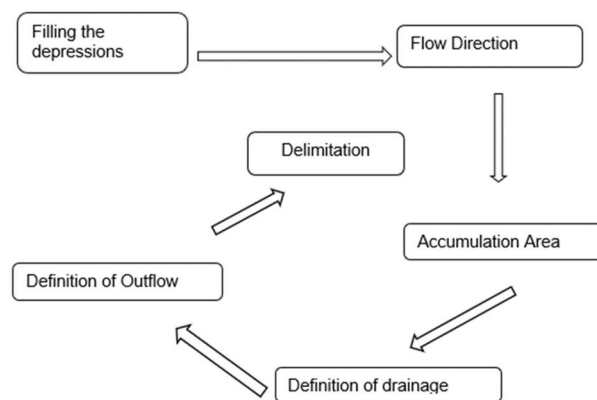


Figure 4: Remote Sensing Data Processing Flowchart.

In the Landsat-5 TM images, the first order polygonal geometric correction was performed, with six control points, having as reference Landsat-8 OLI/TIR images reprojected to the southern hemisphere, with the UTM projection system, Horizontal Datum SIRGAS 2000 Zona 23 South.

Along with the precipitation data, the stations were specialized with the accumulated values in the respective years according to (Table 1) and later performed the interpolation by the IDW method (Inverse Distance Weighting).

Subsequently, Landsat-5 TM and Landsat-8 OLI/TIR images were cut for the basin area, and then processed through radiometric calibration and spectral reflectance, to obtain the biophysical parameters NDVI, SAVI, IAF, and TS.

We performed the calculation of the radiance of bands 3 (red) and band 4 (near infrared) of Landsat-5 /TM. Where radiance is the conversion of the digital number (ND) of each pixel in the image into monochromatic spectral radiance obtained by the equation of Markham et al. (1987):

$$L_{\lambda} = a_i + \frac{b_i - a_i}{255} \cdot ND$$

Where:

$L_{\lambda i}$ represents the solar energy reflected by each pixel per unit area, time, solid angle, measured at the Landsat

satellite level for bands 1, 2, 3, 4, 5 and 7; for band 6, this radiance represents the energy emitted by each pixel. Where a_i and b_i are the minimum and maximum spectral radiance ($W m^{-2} sr^{-1} \mu m^{-1}$), ND is the pixel intensity that corresponds to a range from 0 to 255 and i corresponds to the bands of the satellite under study.

To perform these calculations, the adapted calibration coefficient from Chander et al. (2007). The description of the Landsat 5 TM bands and spectral bands are shown in (Table 2).

Table 2: Description of bands and spectral ranges corresponding to Landsat 5 TM, minimum (a) and maximum (b) calibration coefficients, spectral solar irradiance ($K\lambda$) at the top of the atmosphere (TOA).

Coeficientes de Calibração ($Wm^{-2} \mu m^{-1}$)									
Bandas	Faixa espectral (μm)	01/03/1984 até 04/05/2003		05/05/2003 até 01/04/2007		Após 02/04/2007		$K_2 (\lambda_i)$ ($Wm^{-2} \mu m^{-1}$)	
		a	b	a	b	a	b		
3 (vermelho)	0,63-0,69	-1,17	204,30	-1,17	264,00	-1,17	264,00	1554	0,233
4 (IV-próximo)	0,76-0,90	-1,51	206,20	-1,51	221,00	-1,51	221,00	1036	0,155
6 (IV-termal)	10,4-12,5	1,2378	15,303	1,2378	15,303	1,2378	15,03	-	-

Source: Adapted from Chander et al. (2007).

The NDVI is the most commonly used index for various purposes, including the calculation of leaf area index (ALMEIDA et al., 2015) and aerial biomass (FERRAZ et al., 2004). The NDVI was proposed by Rouse et al. (1973) and is calculated by the difference in reflectance between the near-infrared range and the red range in the visible region according to the equation:

$$DVI = \frac{P_{IVP} - P_V}{P_{IVP} + P_V} \quad (2)$$

Where:

P_{IVP} corresponds to Near Infrared reflectance and P_V corresponds to red reflectance. In the Landsat 5 TM images they are respectively bands 4 and 3, while in the Landsat 8 images, they are bands 5 and 4.

Rouse et al. (1973), normalized the NDVI to the simple ratio to the range -1 to +1 per pixel, so that the closer to +1, the greater the density of vegetation. For ground targets the lower limit becomes approximately zero (0) and the upper limit becomes approximately 0.80.

To minimize the influence of soil reflectance on the NDVI, Huete (1988) incorporated the L factor, giving rise to the SAVI index. This factor promotes an adjustment according to the soil cover, seeking to minimize the effects of soil color on the index results (HUETE, 1988).

According to the equation (HUETE, 1988), SAVI is calculated based on the near infrared (band 4) and red (band 3) bands according to the equation:

$$SAVI = \frac{(1 + L)(p_{iv} - p_v)}{(L + p_{iv} + p_v)} \quad (3)$$

Where.

L – Corresponds to the SAVI adjustment factor, the value of 0.1 used in this study, as recommended by Allen et al. (2002) and Silva et al. (2011).

The Leaf Area Index is defined through the ratio between the leaf area of all vegetation per unit of

area used by this vegetation, being considered as an indicator of biomass of each pixel of the image (ALLEN et al., 2002). The IAF is derived from the SAVI, which is a by-product.

LAI is calculated through the ratio between the leaf area of all vegetation per unit of area used by this vegetation, given by the equation as (ALLEN et al., 2002):

$$IAF = \frac{\ln\left(\frac{0,69 - SAVI}{0,59}\right)}{0,91} \quad (4)$$

The surface temperature is directly linked to the estimation of long wave radiation fluxes and indirectly linked to the surface energy balance fluxes (LIU, 2006).

According to Allen et al. (2002), the surface temperature is obtained, using the inverted Planck equation, valid for a blackbody, in which each pixel does not emit electromagnetic radiation like a blackbody, there is a need to introduce the emissivity of each pixel in the spectral domain. from the thermal band (ϵ_{NB}).

$$T = \frac{K_2}{\ln\left(\frac{\epsilon_{NB} K_1}{L_\lambda} + 1\right)} \quad (5)$$

Where:

K1 and K2 are calibration constants, L_λ Spectral radiance and ϵ_{NB} is the thermal emissivity.

In the Landsat 5 TM images, the thermal band calibration coefficients (band 6) are obtained from the MTL (Metadata), where K1 = 607.76 and K2=1260.56. In the Landsat 8 OLI/TIR images, the thermal band calibration coefficients (band 10) are also obtained in the MTL (Metadata), but with different values, where K1 = 1321.08 and K2 =774.89.

Being the emissivity ϵ_{NB} obtained by the equation:

$$\epsilon_{NB} = 0,97 + 0,0033 \cdot IAF \quad (6)$$

The Radiance of Landsat 8 was obtained by the equation:

$$L_\lambda = M_L Q_{cal} + A_L \quad (7)$$

Where:

L_λ is the spectral radiance of the sensor; M_L is the band scaling multiplicative factor $10= 3.3420E-04$; Q_{cal} is the quantized value calibrated by the pixel in DN = image of band 10; A_L band-specific additive scaling factor $10= 0.10000$.

After processing the images, the thematic maps of the biophysical indices (NDVI, SAVI, IAF and TS) for the years 1984, 1994, 2004 and 2017 were generated. These indices will support the analysis of the space-time dynamics that occurred in the River Basin of Rio de Janeiro – BA.

RESULTS AND DISCUSSION

In the process of identifying and quantifying the percentages of green cover distributed in the basin area, the vegetation indices were estimated: (NDVI, SAVI and IAF). The Figure 5 presents the statistical values on the dates under analysis, highlighting the means and standard deviation. The interpretive analysis shows mean values ranging from 0.23% (242/2004) to 0.35% (230/1994) and, with standard deviation ranging from 0.12% (242/2004) to 0.48% (230 /1994), with an amplitude of 36%. These values portray the different uses

of land cover, as each target has a different spectral response. In this area, the native Cerrado vegetation, water bodies, exposed soil, rainfed and irrigated agriculture stand out.

The highest averages are concentrated in the dates 267/1984 and 230/1994, period in which the amount of moisture in the soil was higher due to the precipitation accumulated before the recording of the scenes.

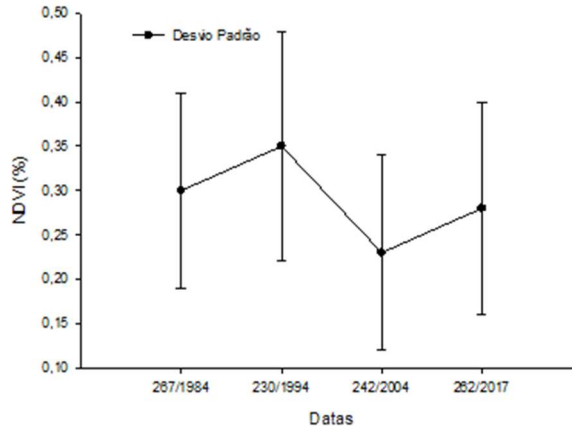


Figure 5: Mean values and standard deviation of NDVI in 276/1994, 230/1994, 242/2004 and 262/2017.

Figure 6 represents the spatial distribution of NDVI values for the dates under analysis. The highest values were then represented in the interval $> 0.55\%$, highlighting the features with a high percentage of vegetation, in the green shade. The areas with the lowest values are represented in tuscan red in the range $< -0.26\%$. Values close to zero are represented in the range between -0.05% to 0.14% , in beige, which according to the literature can be exposed soil.

In the analysis of the images, it can be seen that the years 267/1984 and 230/1994 have the highest NDVI values. In the years 242/2004 and 262/2017 the values with the lowest percentage are concentrated in the western portion, with a gradual loss of green cover in the multitemporal analysis. This discrepancy between the dates in the analysis may be related to precipitation as observed in figure 7 (Precipitation accumulated in the three months prior to the satellite passage) the volumes accumulated in the first two years demonstrate the presence of moisture in the soil, causing the spectral responses of green cover are more representative. It is important to emphasize that other variables, such as deforestation, were not taken into account.

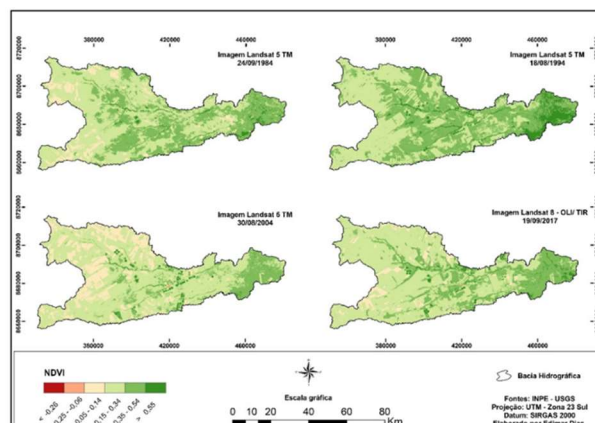


Figure 6: NDVI thematic letter on dates 276/1994, 230/1994, 242/2004 and 262/2017.

General literature data characterize the temporal variation of NDVI related to agricultural practices.

The study highlighted a 34% reduction in the class with higher density native vegetation (Figure 5).

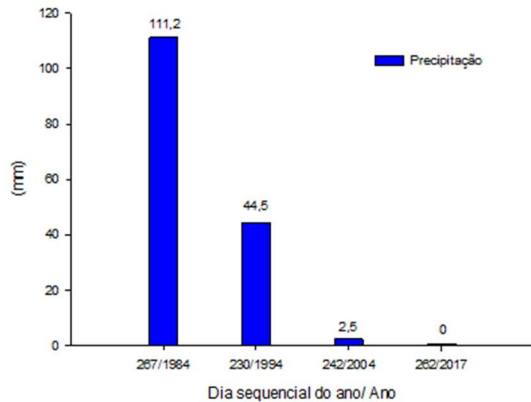


Figure 7: Precipitation accumulated in the three months before the satellites passed.

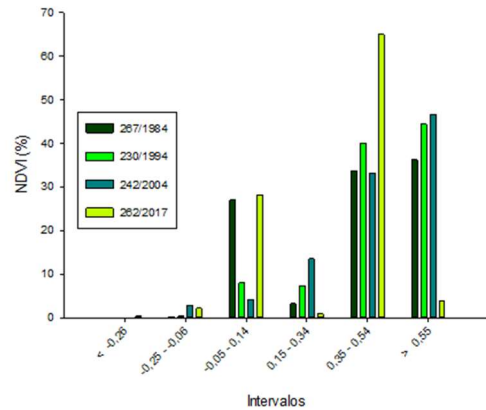


Figure 8: Percentage of NDVI classes for the dates under analysis.

Figure 8 shows the percentages of pixels in each NDVI class for the dates under analysis. It is observed in figure 8 that the largest spatial distribution in all scenes was found in the range 0.35% - 0.54%, highlighting the dates 267/1984 to 242/2004 with values above 33% and the year 262/ 2017 with 76.61%. In the interval > 0.55%, which corresponds to areas with the highest density of vegetation, it was found that the year 242/2004 had the highest percentage (46.51%), while the year 262/2017 showed the lowest value 2.51 %.

The SAVI is an index that takes into account the effects of the exposed soil in the analyzed images, serving as an adjustment of the NDVI, when the surface is not completely covered by vegetation. Figure 9 highlights the mean values and standard deviation of SAVI.

Figure 9 shows the decline in average values in the first years up to date 242/2004, which had the lowest average percentage between the periods 0.16%. The highest average percentage occurred in 267/1984 with 0.24%. Thus, there is an average percentage range of 0.08% with the percentage of standard deviation oscillating in the scenes between 0.06% and 0.30%.

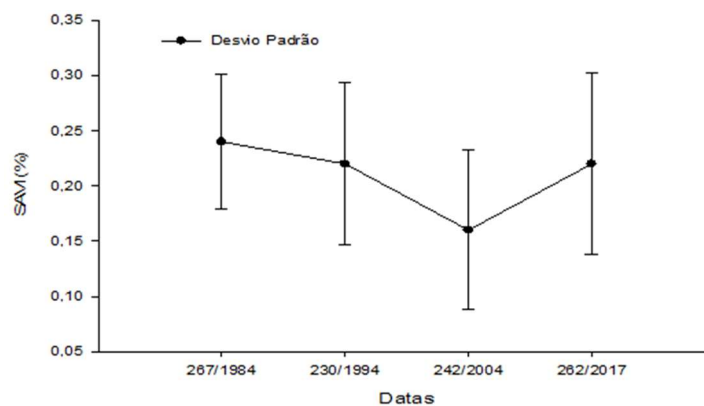


Figure 9: Mean values and standard deviation of SAVI on the dates under analysis.

The results obtained from the SAVI highlighted the areas of exposed soil that were not evidenced in the spatial distribution of the NDVI. In the years 242/2004 and 262/2017 there was an emphasis on the distribution of pixels close to zero in the western portion, represented in the class <10, indicating areas with exposed soil (Figure 9). Once it is a dry period in the study area, the spatial distribution of the interval > 0.51% represented in green highlights the areas of veredas and irrigation with central pivot.

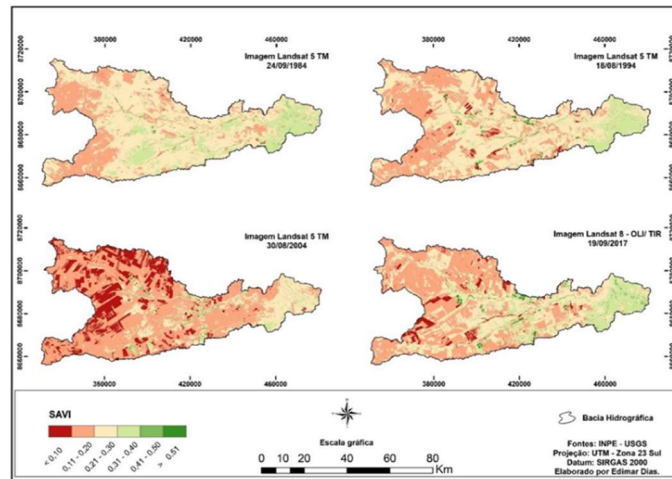


Figure 9: SAVI thematic letter on the dates under review.

Figure 10 shows the percentage of pixels in each SAVI class, where the smallest spatial distribution is in the range >0.51%, except for date 262/2017, which presented 9.56%. Comparing with the NDVI (Figure 8), the exact opposite occurred in relation to the interval >0.55%. This is in part because SAVI has a ground-adjusted correction factor. The interval between 0.11% and 0.20% presented the highest percentage of spatial distribution of the scenes in 242/2004 with 39.07%, justifying the increase in areas with exposed soil previously mentioned in the western portion of the respective date. The lowest percentage of distribution occurred in the interval >0.51% on date 242/2004 with 0.20%.

Huete et al. (1988) found that the sensitivity of vegetation indices in relation to the background material (soil) is greater in canopies with average levels of vegetation cover (50% of green cover) through a constant “L” introduced by them in the experimental measurements. of reflectances, calculated for the near-infrared and red bands. The constant “L” has the function of minimizing the effect of the soil on the result of the index, with values ranging from -1.5 for areas without vegetation to 1.5 in areas with the presence of some vegetation. The results presented in Figure 10 corroborate the findings of Huete et al. (1988).

LAI is an indicator of the biomass present in each pixel of the images. Figure 11 shows the mean values and standard deviation of the LAI. Figure 11 shows a variation of 0.10% between the average values of the scenes. The highest values found were on dates 230/1994 and 262/2017 with 0.36%, while the lowest value occurred on 242/2004 with 0.26%. The standard deviation ranged between 0.14% on the date 242/2004 and 0.54% on 262/2017.

Figure 12 represents the spatial distribution of the IAF, where it is possible to see in all the scenes the values of the intervals 0.63% - 0.82% is concentrated in the eastern portion of the basin, as well as in riparian forest areas and pivot of irrigation, these intervals are represented in medium green hue. It is evident

that the western portion of the basin has the predominance of the intervals between 0.03% to 0.22% with the salmon hue.

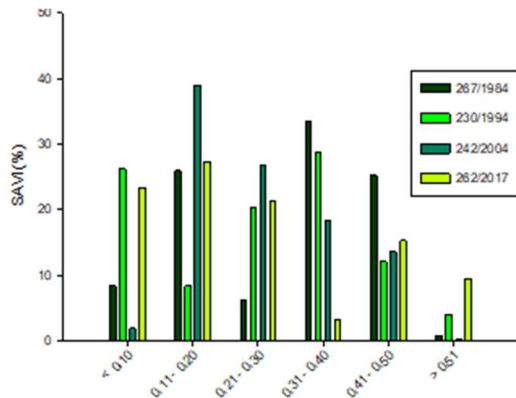


Figure 10: Percentage of SAVI classes for the dates under analysis.

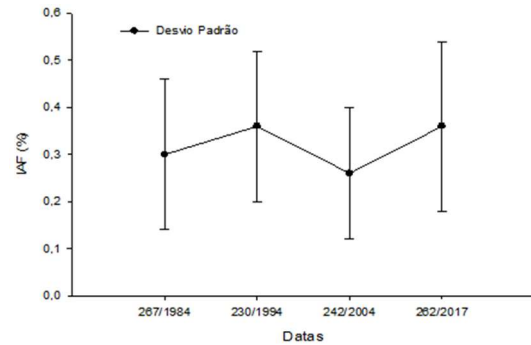


Figure 11: Mean values and standard deviation of the IAF on the dates under analysis.

Figure 13 shows the percentage of pixels in each IAF class. It is observed in figure 13, that the class of intervals from 0.43% to 0.62% presented a greater spatial distribution in 26/7/1984 with 42.84%, whereas in the following dates there was a reduction in the values. In the range between 0.63% to 0.82%, it represents features with high vegetation density. The increase in values IAF in all scenes stands out, where in 26/7/1984 the percentage was 2.73%, rising to 34.25% in 26/2/2017.

The demonstration of how much the vegetation cover is susceptible to the variation of water in the soil, can also be understood through the IAF. These authors confirmed that the change in LAI of the cerrado pasture is directly influenced by the seasonal fluctuation of the water level in the soil. This evidence of LAI is justified by the greater absorption of radiation in the rainy season, characteristic of a greater growth of vegetation cover. According to Toniol et al. (2017), the class discrimination in Cerrado is generally facilitated in the dry season, requiring the use of a greater number of metrics (spectral bands or vegetation indices) in the classification of vegetation during the rainy season due to greater spectral confusion with the greater homogenization between the gradient of classes in this period. The LAI data obtained in this study corroborate the approach of Toniol et al. (2017).

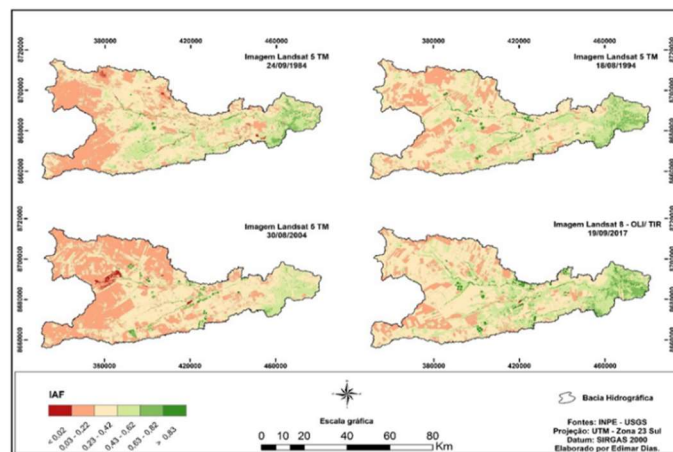


Figure 12: IAF thematic letter on the dates under review.

Figure 14 shows the means and standard deviation of surface temperatures for the dates under analysis. It is possible to verify that the highest average recorded in all scenes occurred on date 262/2017 with 37°C, with the standard deviation oscillating approximately between 36.1°C and 39.9°C. The lowest average was recorded in 230/1994, 25°C, with standard deviation ranging between 23.2°C and 26.8°C. On the date 242/2004, the greatest variation around the mean was recorded, with an amplitude of 6°C.

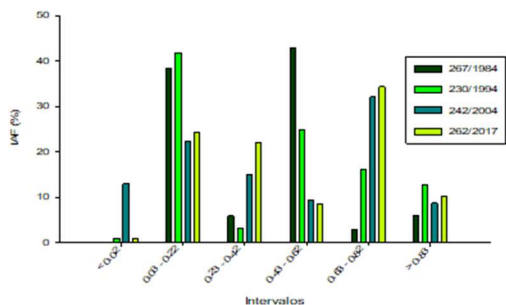


Figure 13: Percentage of IAF classes for the dates under analysis.

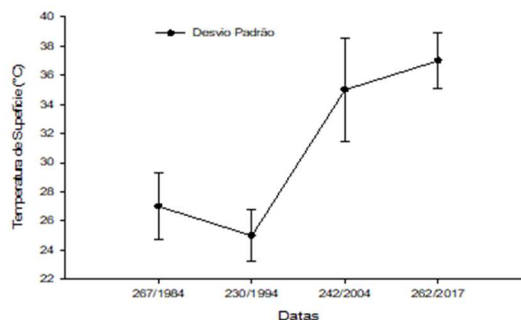


Figure 14: Mean values and standard deviation of surface temperature on the dates under analysis.

This amplitude between the values of the maximum and minimum averages is directly related to the three months that preceded the passage of the satellites, since, on the dates 267/1984 and 230/1994, there was a significant accumulation of precipitation, as can be seen in Graph 2.

According to Borges et al. (2011), this amplitude may be associated with different weather conditions during the acquisition of images, which reinforces the amount of moisture present on the surface. Figure 15 represents the spatial distribution of surface temperature on the dates under analysis, where it is possible to contact the highest values in the red shade, with an interval $>38^{\circ}\text{C}$, represented more expressively on the dates 242/2004 and 262/2017. The year 1984 had the lowest surface temperatures. This fact can be directly related to the volume of accumulated precipitation and the presence of native vegetation of Cerrado, because in this period the process of expansion of the agricultural frontier in the region was starting.

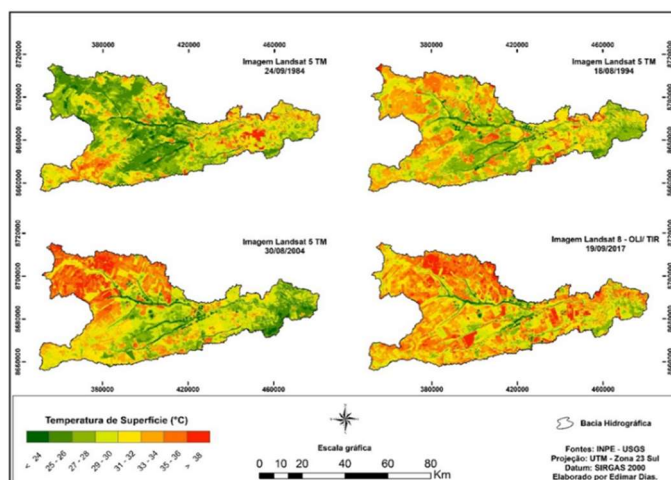


Figure 15: Thematic chart of Surface Temperature on the dates under analysis.

Figure 16 shows the percentage of TS classes for the dates under analysis. It can be seen in figure 16, where the highest percentage occurred in the interval $31^{\circ}\text{C} < T < 32^{\circ}\text{C}$ on the date 242/2004, with 29.20%.

While the lowest was 0.09% in the range > 38°C on the date 267/1984.

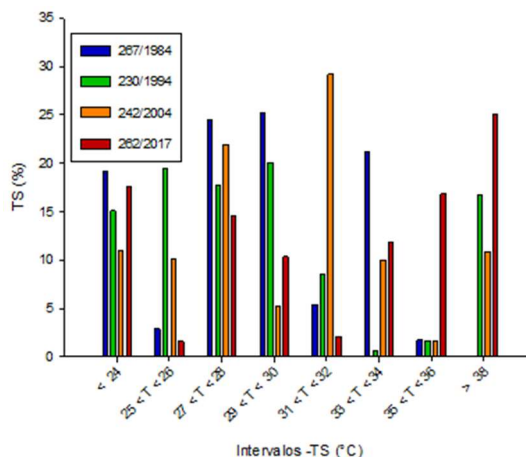


Figure 16: Percentage of TS classes for the dates under analysis.

Borges et al. (2011) in a study in western Bahia using Landsat images obtained an average surface temperature of approximately 22°C in the year 1984, while in the other years analyzed (1992, 2000 and 2008) the average temperature was approximately 35°C. These authors verified in this period the suppression of the natural vegetation of Cerrado and consequently the exposition of the soil, whether for agriculture or for pasture. These values agree with the present study, which showed an increase in surface temperature from 1984 to 2017. It is noteworthy, however, that the year 1994 showed a small reduction of approximately 2°C compared to 1984. This can be resulting from local climate change related to the 1994’s rainfall.

CONCLUSIONS

The study evidence that from similar climatic conditions (dry period) it was possible to compare the results obtained from the processing of images from the years 1984, 1994, 2004 and 2017 and to verify multitemporal changes in the vegetation indices in the percentages of classes and values.

The amount of moisture present in the soil due to the accumulated precipitation was directly related to the results obtained, mainly in the years 1984 and 1994, which presented the highest values of NDVI. While in the years 2004 and 2017, the values point to a lower percentage in the eastern portion of the basin, with a gradual loss of green cover in the multitemporal analysis.

The SAVI was compared with the NDVI once it showed areas that had exposed soil from mechanized agriculture implemented in the Rio de Janeiro Basin from the 1980s onwards. The biomass indicator presents in each pixel of the IAF images showed similarities to SAVI, showing the areas in the eastern portion of the basin as the highest vegetative percentages.

It was found that the surface temperature in the years 1984 and 1994 were lower. This fact may be related to the accumulated precipitation and areas of native vegetation. However, there was a significant increase in temperature in 2004 and 2017, respectively, 35 and 37°C. Indicating the suppression of natural savanna vegetation related to the expansion of agriculture.

The results obtained through the biophysical parameters (NDVI, SAVI, IAF and Ts) portray the

different uses of land cover. Characterizing the spectral responses of different types of land cover in the surroundings of the Rio de Janeiro Bahia/Brazil River Basin, such as native Cerrado vegetation, water bodies, exposed soil, rainfed and irrigated agriculture.

The relationship between energy flows in the Cerrado biome of the Rio de Janeiro Basin BA/Brazil proved to be representative compared to the variation of vegetation in the period from 1984 to 2017, favoring local and regional environmental and climate analysis. Changes in vegetation and surface temperature indices directly reflected the variation of available water in the environment, characterizing a strong relationship between seasonality in the data and the Cerrado deforestation.

This study shows that the history of transformations that occurred in the Cerrado of the Rio de Janeiro Basin Bahia/Brazil from 1984 to 2017, mainly related to the expansion of agricultural frontiers that occurred, systematically helps to identify significant environmental and climatic damages related to the habitat fragmentation, decreased biodiversity, soil erosion and ecosystem degradation.

REFERENCES

- ALENCAR, A.; SHIMBO, J. Z.; LENTI, F. L.; MARQUES, C. B.; ZIMBRES, B.; ROSA, M.; ARRUDA, V.; CASTRO, I.; RIBEIRO, J. P. F. M.; VARELA, V.; ALENCAR, I.; PIONTEKOWSKI, V.; RIBEIRO, V.; BUSTAMANTE, M. M. C.; SANO, E. E.; BARROSO, M.. Mapping three decades of changes in the Brazilian Savanna native vegetation using Landsat data processed in the Google Earth engine platform. **Remote Sensing**, v.12, n.924, 2020.
- ALLEN, R. G.; TASUMI, M.; TREZZA, R.; SEBAL, Surface Energy Balance Algorithms for Land. **Advance training and users manual: Idaho Implementation, VERSION 1.0**. 2002.
- ALMEIDA, A. Q.; RIBEIRO, A.; DELGADO, R. C.; RODY, Y. P.; OLIVEIRA, A. S.; LEITE, F. P.. Índice de área foliar de Eucalyptus estimado por índices de vegetação utilizando imagens TM – Landsat 5. **Floresta e Ambiente**, v.22, n.3, p.368-376, 2015.
- ARGEMIRO, L.; ARAÚJO, A. L.; SILVA, M. T.; SILVA, B. B.; SANTOS, C. A. C.; DANTAS, M. P.. Análise das mudanças de parâmetros biofísicos sobre o nordeste brasileiro de 2002 a 2011 com dados modis. **Revista Brasileira de Meteorologia**, v.33, n.4, p.589, 2018.
- BEZERRA, J. N. M.; MOURA, G. B. A. M.; SILVA, B. B.; LOPES, P. M. O.; SILVA, E. F. F.. Parâmetros biofísicos obtidos por sensoriamento remoto em região semiárida do estado do Rio Grande do Norte, Brasil. **Revista Brasileira de Engenharia Agrícola e Ambiental**, v.18, n.1, p.73-84, 2014.
- BORGES, E. F.; ANJOS, C. S.; BAPTISTA, G. M. M.. Análise Multitemporal da temperatura de superfície no oeste da Bahia. In: SIMPÓSIO BRASILEIRO DE SENSORIAMENTO REMOTO, 15. **Anais**. Curitiba, 2011.
- CHANDER, G.; MARKHAM, B. L.; BARSÍ, J. A.. Revised Landsat -5 Thematic Mapper Radiometric Calibration. **IEEE Geoscience and Remote Sensing Letters**, v.4, n.3, p.490-494, 2007.
- CUNHA, E. R.; SANTOS, C. A. G.; SILVA, R. M.; PANACHUKI, E.; OLIVEIRA, P. T. S.; OLIVEIRA, N. S.; FALCÃO, K. S.. Assessment of current and future land use/cover changes in soil erosion in the Rio da Prata basin (Brazil). **Sci. Total Environ.**, v.807, p.151811, 2022.
- EMBRAPA. Empresa Brasileira de Pesquisa Agropecuária. **Boletim Geomorfológico do Município de Barreiras, Oeste Baiano, escala 1: 100.000**. Planaltina: EMBRAPA, 2010.
- FALEIRO, F. G.; FARIAS NETO, A. L.. **Savanas: demandas para a pesquisa**. Planaltina: Embrapa Cerrados, 2009.
- FERRAZ, Z. M. L.. A produção de grãos na Região Oeste da Bahia. **Revista Bahia Agrícola**, v.6, n.3, p.3-10, 2004.
- FONSECA, C. A. B.; AL-ANSARI, N.; SILVA, R. M.; SANTOS, C. A. G.; BILEL ZEROUALI, B.; OLIVEIRA, D. B.; AHMED ELBELTAGI, A. A.. Investigating Relationships between Runoff–Erosion Processes and Land Use and Land Cover Using Remote Sensing Multiple Gridded Datasets. **ISPRS Int. J. Geo-Inf.**, v.11, n.272, 2022.
- HILL, M. J.. Vegetation index suites as indicators of vegetation state in grassland and savanna: An analysis with simulated SENTINEL 2 data for a North American transect. **Remote Sensing of Environment**, v. 137, p. 94–111, out. 2013.
- HUETE, A. R.. A soil adjusted vegetation index (SAVI). **Remote Sensing of Environment**, v.25, n.3, p.295-309, 1988.
- LIU, W. T. H.. **Aplicações de Sensoriamento Remoto**. Campo Grande: UNIDERP, 2006.
- LOPES, H. L.; CANDEIAS, A. L. B.; ACCIOLY, L. J. O.; SOBRAL, M. C. M.; PACHECO, A. P.. Parâmetros biofísicos na detecção de mudanças na cobertura e uso do solo em bacias hidrográficas. **Revista Brasileira de Engenharia Agrícola e Ambiental**, v.14, p.1210-1219, 2010.

MARKHAM, B. L.; BAKER, J. L.. Thematic mapper bandpass solar exoatmospherical irradiances. **Int. Journal of Remote Sensing**, v.8, n.3, p.517-523, 1987.

MENDONÇA, J. O.. O potencial de crescimento da produção de grãos no Oeste da Bahia. **Revista Bahia Agrícola**, v.7, n.2, 2006.

MITTERMEIER, R. A.; TURNER, W. R.; LARSEN, F. W.; BROOKS, T. M.; GASCON, C.. Global biodiversity conservation: the critical role of hotspots. In: **Biodiversity Hotspots**. Springer: Berlin; Heidelberg, 2011. p.3-22.

OLIVEIRA, M. T.; CASSO, H. L. G.; GANEM, K. A.; DUTRA, A. C.; PRIETO, J. D.; ARAI, E.; SHIMABUKURO, Y. E.. Mapping the Cerrado's vegetation cover: a review of remote sensing initiatives. **Rev. Bras. Cartogr**, v.72, n.50, 2020.

REIS, S. L. S.. **Desenvolvimento e natureza**: a dinâmica de ocupação do cerrado e repercussões ambientais na região agroexportadora do oeste baiano. Salvador: Instituto de geociências; Universidade Federal da Bahia, 2014.

ROCHA, G. F.; FERREIRA, L. G.; FERREIRA, N. C.; FERREIRA, M. E.. Detecção de desmatamentos no bioma Cerrado entre 2002 e 2009: Padrões, tendências e impactos. **Revista Brasileira de Cartografia**, v.3, p.341-349, 2011.

ROUSE, J. W.; HAAS, R. H.; SCHELL, J. A.; DEERING, D. W.. Monitoring vegetation systems in the great plains with ERTS. In: EARTH RESOURCES TECHNOLOGY SATELLITE-1 SYMPOSIUM, 3. **Annals**. Washington, 1973. p.309-317.

SANO, E. E.; ROSA, R.; BRITO, J. L. S.; FERREIRA, L. G.. Land cover mapping of the tropical savanna region in Brazil. **Environ. Monit. Assess**, v.166, p.113-124, 2010.

SANO, E. E.; ROSA, R.; SCARAMUZZA, C. A. M.; ADAMI, M.; BOLFE, E. L.; COUTINHO, A. C.; ESQUERDO, J. C. D. M.; MAURANO, L. E. P.; NARVAES, I. S.; OLIVEIRA FILHO, F. J. B.. Land use dynamics in the Brazilian Cerrado in the period from 2002 to 2013. **Pesqui. Agropecuária Bras.**, v.54, 2019.

SILVA, J. L. B.; MOURA, G. B. A.; SILVA, E. F. F.; LOPES, P. M. O.; SILVA, T. T. F.; LINS, F. A. C.; SILVA, D. A. O.; ORTIZ, P. F. S.. Spatial-temporal dynamics of the Caatinga vegetation cover by remote sensing in municipality of the Brazilian semi-arid. **Revista Brasileira de Ciências Agrárias**, v.14, p.1-10, 2019.

SILVA, B. B.; BRAGA, A. C.; BRAGA, C. C.. Balanço de radiação no perímetro irrigado São Gonçalo/PB mediante imagens orbitais. **Revista Caatinga**, v.24, p.145-152, 2011.

STRASSBURG, B. B. N.; BROOKS, T.; BARBIERI, R. F.; IRIBARREM, A.; CROUZEILLES, R.; LOYOLA, R.; LATAWIEC, A. E.; OLIVEIRA FILHO, F. J. B.; SCARAMUZZA, C. A. M.; SCARANO, F. R.. Moment of truth for the Cerrado hotspot. **Nat. Ecol. Evol.**, v.1, n.99, 2017.

TARTARI, R.; MACHADO, N. G.; ANJOS, M. R. D.; CUNHA, J. M. D.; MUSIS, C. R. D.; NOGUEIRA, J. D. S.; BIUDES, M. S.. Evaluation of biophysical indices from TM Landsat 5 images in heterogeneous landscape in Southwestern Amazon. **Revista Ambiente & Água**, v.10, p.943-953, 2015.

TONIOL, A. C.; GALVÃO, L. S.; PONZONI, F. J.; SANO, E. E.; AMORE, D. J.. Potential of hyperspectral metrics and classifiers for mapping Brazilian savannas in the rainy and dry seasons. **Remote Sensing Applications: Society and Environment**, v.8, p.20-29, 2017.

Os autores detêm os direitos autorais de sua obra publicada. A CBPC – Companhia Brasileira de Produção Científica (CNPJ: 11.221.422/0001-03) detêm os direitos materiais dos trabalhos publicados (obras, artigos etc.). Os direitos referem-se à publicação do trabalho em qualquer parte do mundo, incluindo os direitos às renovações, expansões e disseminações da contribuição, bem como outros direitos subsidiários. Todos os trabalhos publicados eletronicamente poderão posteriormente ser publicados em coletâneas impressas ou digitais sob coordenação da Companhia Brasileira de Produção Científica e seus parceiros autorizados. Os (as) autores (as) preservam os direitos autorais, mas não têm permissão para a publicação da contribuição em outro meio, impresso ou digital, em português ou em tradução.